# Oridonin Inhibits Hepatic Stellate Cell Proliferation and Fibrogenesis

**Fredrick J. Bohanon, MD**[#][a], **Xiaofu Wang, BS**[#][a], **Chunyong Ding, PhD**[b], **Ye Ding, PhD**[b], **Geetha L. Radhakrishnan, MD**[c], **Cristiana Rastellini, MD**[a], **Jia Zhou, PhD**[b], and **Ravi S. Radhakrishnan, MD**[a,c]

[a]Department of Surgery, University of Texas Medical Branch, 301 University Blvd., Galveston, TX, 77555, USA

[c] Department of Pediatrics, University of Texas Medical Branch, 301 University Blvd., Galveston, TX, 77555, USA

[b]Chemical Biology Program, Department of Pharmacology and Toxicology, University of Texas Medical Branch, 301 University Blvd., Galveston, TX, 77555, USA

[#] These authors contributed equally to this work.

## Abstract

**Introduction**—Liver fibrosis is a common response to liver injury and, in severe cases, leads to cirrhosis. The hepatic stellate cells (HSC) become activated after liver injury and play a significant role in fibrogenesis. The activated HSC is characterized by increased proliferation, overexpression of α-smooth muscle actin (α-SMA), and excessive production of extracellular matrix (ECM) proteins. Oridonin, a naturally occurring diterpenoid, has been shown to induce apoptosis in liver and gastric cancer cells. However, its effects on HSC are unknown.

**Methods**—We tested the effects of oridonin on the activated human and rat hepatic stellate cell lines LX-2 and HSC-T6 as well as the human hepatocyte cell line C3A. Transforming growth factor β1 (TGF-β1) was used to stimulate LX-2 cells.

**Send correspondence to:** Ravi S. Radhakrishnan Department of Surgery, The University of Texas Medical Branch, 301 University Boulevard, Galveston, Texas 77555-0353 Telephone: (409) 772-5666 FAX: (409) 772-*4253*rsradhak@utmb.edu.

**Results**—Oridonin significantly inhibited LX-2 and HSC-T6 proliferation. In contrast, Oridonin had no anti-proliferative effect on C3A cells at our tested range. Oridonin induced apoptosis and S phase arrest in LX-2 cells. These findings were associated with an increase in p53, p21, p16, and cleaved PARP, and with a decrease in Cdk4. Oridonin markedly decreased expression of α-SMA and ECM protein type I collagen and fibronectin, blocked TGF-β1-induced Smad2/3 phosphorylation and type I Collagen expression.

**Conclusions**—Oridonin induces apoptosis and cell cycle arrest involving the p53/p21 pathway in HSC, and appears to be non-toxic to hepatocytes. In addition, oridonin suppressed endogenous and TGF-β-induced ECM proteins. Thus, oridonin may act as a novel agent to prevent hepatic fibrosis.

## Keywords

## 1. Introduction

Hepatic fibrosis is a final common pathway of both acute and chronic diseases including biliary atresia, hepatitis, primary sclerosing cholangitis, and primary biliary cirrhosis leading to cirrhosis. The economic burden of cirrhosis resulted in $10.6 billion in direct and indirect costs in 2004 and is expected to rise in the next decade [1]. Preventing or inhibiting the progression of fibrosis leading to cirrhosis may reduce the economic burden and, more importantly, may reduce the decline in health-related quality of life. The primary effector cell type for hepatic fibrosis is the hepatic stellate cells (HSC) [2]. HSC reside within the space of Disse and have their dendritic processes interacting with hepatocytes and sinusoidal endothelial cells [3]. HSC undergo trans-differentiation into a myofibroblast-like phenotype upon activation via numerous stimuli, such as transforming growth factorβ1 (TGF-β1), lipopolysaccharide (LPS)/toll-like receptors, tissue hypoxia, platelet-derived growth factors (PDGF), nicotinamide adenine dinucleotide phosphate-oxidase (NADPH), and the renin-angiotensin system [4, 5]. HSC activation is characterized by the overexpression of α-smooth muscle actin (α-SMA) [6]. Activated HSC induce fibrosis via increased proliferation, excessive deposition of ECM, and expression of profibrogenic cytokines [7, 8]. Therefore, inhibition of activated HSC has become an area of increasing clinical interest.

Natural products have attracted much attention since they have served as major sources of chemical diversity for biomedical agents or lead candidates while driving pharmaceutical discovery. Oridonin is an active compound isolated from *Rabdosia rubescens*, which is a herbal medicine that is traditionally used as an anti-inflammatory, antibacterial, and anticancer agent in local folk medicine in East Asia [9]. From the 1970s in China, isolated oridonin is used alone or in combination with other drugs to treat swelling of the throat, insect bites, tonsillitis, and different cancers including liver, esophagus, gastric, and breast [10-15]. Zhou and colleagues reported that oridonin showed significant antileukemic and organ protective effects without obvious adverse reaction. Their results revealed that oridonin treatment markedly reduced disseminated disease and prevented destruction of tissue architectures caused by leukemia in liver, bone marrow, and spleen [16]. However, the effect of oridonin on liver fibrosis remains unknown.

In the present study, we determine the role of oridonin on hepatic fibrosis using the activated human and rat hepatic stellate cell lines LX-2 and HSC-T6. Since these cell lines retain key features of primary HSC, they have been adopted as useful tools for liver fibrosis research [17].

## 2.Materials and Methods

### 2.1. Reagents

All cell culture mediums and trypsin were purchased from Life Technology Corp. (Carlsbad, CA). Oridonin and antibody against α-smooth muscle actin (α-SMA) (Cat#5228) were purchased from Sigma-Aldrich Co. LLC. (St. Louis, MO). TGF-β1 was purchased from R&D Systems Inc. (Minneapolis, MN). Propidium iodide was from MP Biomedicals, LLC (Solon, OH). Antibodies against Fibronectin (sc-6952) and Cdk4 (sc-749) were purchased from Santa Cruz Biotechnology Inc (Santa Cruz, CA). Anti-Collagen Type I polyclonal antibody (600-401-103) was from Rockland Immunochemicals Inc. (Gilbertsville, PA). GAPDH antibody (10R-G109A) was from Fitzgerald Industries (Concord, MA). Anti-p21 (Cat#556431) and p16 (Cat#551153) were from BD Biosciences (San Jose, CA). Anti-p53 (Cat#2527), cleaved PARP (Cat#5625), cleaved caspase-9 (Cat#9505) and phospho-Smad2/3 (Cat#8828) were from Cell Signaling Technology Inc. (Danvers, MA).

### 2.2. Cell culture

The human immortalized HSC line LX-2 and rat immortalized HSC line HSC-T6 were a gift from Dr. Scott Friedman (Mount Sinai Medical Center, New York) and cultured at 37° C with 5% $CO_2$ in Dulbecco's modified Eagle's medium (DMEM) with a high glucose concentration (4.5 g/L) supplemented with 5% fetal bovine serum (FBS), 1% penicillin/ streptomycin. Human hepatocyte cell line C3A was obtained from American Type Cell Culture (ATCC, Manassas, VA), and maintained in DMEM medium containing 10% FBS. All experiments were performed on cells within 6 weeks of culture from liquid nitrogen.

### 2.3. Western immunoblotting

Whole cell extracts were prepared using RIPA buffer (Thermo Fischer Scientific, Inc., Waltham, MA) with 1% Halt protease inhibitor cocktail and 1% Halt phosphatase inhibitor cocktails (Thermo Fischer Scientific, Inc., Waltham, MA). The protein concentration was measured and quantified by the Bradford method. 10-30 g of protein were fractionated by sodium dodecyl sulfate-polyacrylamide gel electrophoresis (SDS-PAGE) (Life Technologies Corporation, Grand Island, NY) under denaturing conditions and then electro-transferred to a polyvinylidene fluoride (PVDF) membrane. After being blocked with Blocking buffer (LI-COR, Inc., Lincoln, NE) the membrane was probed with the indicated primary antibody (Ab) diluted with blocking buffer. Membranes were washed three times with Phosphate buffered saline with 0.1% Tween 20 (PBST), and incubated 1 hour with IRDye 680-conjugated anti-mouse or IRDye 800-conjugated anti-rabbit Ab (LI-COR, Inc., Lincoln, NE). Finally, the membranes were washed three times with PBST, and signals were scanned and visualized by Odyssey Infrared Imaging System (LI-COR, Inc., Lincoln, NE). Densitometric analysis was performed on the proteins of interest and normalized to GAPDH by LI-COR Image Studio software (LICOR, Inc., Lincoln, NE).

### 2.4. Cell Death Detection ELISA Assay

$8 \times 10^3$ cells/well were seeded into 96-well plates. Next day, after reaching 70-80% confluence, cells were replaced with fresh complete medium and treated as indicated. Apoptosis was determined using a Cell Death Detection ELISA Kit (product # 11 774 425 001, Roche Diagnostics Corp. Indianapolis, IN) following manufacturer's protocol. Assay was performed in duplicate and repeated twice.

### 2.5. Detection of Yo-Pro-1 Uptake.

For the detection of apoptosis by Yo-Pro-1 (Life Technologies Corporation, Grand Island, NY), cells were seeded in 24-well plates with $0.25 \times 10^5$ cells/well. Next day, cells were treated with 10 M of Oridonin for 12 hours. After being washed with PBS, cells were incubated with 1 M of Yo-Pro-1 for 1 hour. Yo-Pro-1 uptake was determined by confocal microscope (Nikon Instruments Inc. Melville, NY).

### 2.6. Alamar Blue / Cell Viability Assay

We selected the Alamar Blue-based cytotoxicity assay as our primary assay because Alamar Blue is a non-toxic metabolic indicator of viable cells that becomes fluorescent upon mitochondrial reduction, does not involve washing steps, and is more sensitive than other methods [18, 19]. $3 \times 10^3$ cells/well of LX-2 cells, $4 \times 10^3$ cells/well of HSC-T6 cells, or $5 \times 10^3$ cells/well of C3A cells in 100 L complete medium were seeded into 96-well plates. Next day, cells reached 50-60% confluence and were replaced with fresh complete medium and treated as indicated for 48 hours (or 24 hours, 72 hours). Alamar blue stock solution (Life Technologies Corporation, Grand Island, NY) was diluted to 1:1 with culture medium and a volume of 25 L/well was transferred into the assay plate for final concentration of 10% alamar blue. The plate was returned to incubator for another 4 hours. Fluorescence intensity was monitored using a SpectraMax M2 microplate reader (Molecular Devices, LLC, Sunnyvale, CA) with excitation and emission wavelengths set at 540 and 590 nm, respectively. Assay was performed triplicate and repeated at least three times.

### 2.7. Cell Cycle Analysis by Flow Cytometry

Nuclear DNA content was measured by using propidium iodide staining and fluorescence-activated cell sorter analysis. Briefly, $2 \times 10^6$ adherent cells were trypsinized, washed with phosphate-buffered saline, resuspended in a low-salt stain solution (3% polyethylene glycol 8000, 50 g of propidium iodide per mL, 0.1% Triton X-100, 4 mM sodium citrate, 180 units of RNase A per mL), and incubated at 37°C for 20 minutes. An equal volume of high-salt stain solution (3% polyethylene glycol 8000, 50 g of propidium iodide per ml, 0.1% Triton X-100, and 400 mM sodium chloride) was then added to the cell suspension. Propidium iodide-stained nuclei were stored at 4°C at least 3 hours before fluorescence-activated cell sorter analysis using BD FACSCanto II flow cytometer (Becton, Dickinson and Company, Franklin Lakes, NJ) at University of Texas Medical Branch Flow Cytometry and Cell Sorting Core Facility. ModFit LT for Win32 software was used for data analysis (Verity Software House, Inc., Topsham, ME).

### 2.8. Electrophoretic Mobility Shift Assay (EMSA)

LX-2 cells were pretreated for 2 hours with oridonin prior to introduction of TGF-β as indicated. The nuclear extracts were prepared from LX-2 cells using NE-PER Nuclear and Cytoplasmic Extraction Reagents (Thermo Fischer Scientific, Inc., Rockford, IL) according to the manufacturer's protocol. 10 μL of nuclear extracts were incubated with a $^{32}$P-γATP-labeled oligonucleotide ($5 \times 10^4$cpm) (PerkinElmer Inc., Waltham, MA) containing Smad SBE binding sites (sc-2603, Santa Cruz Biotechnology, Inc.) and 4 μL of 5x Binding Buffer (Promega Corporation, Madison, WI) in a final volume of 20 μL for 15 minutes at room temperature. The reaction mixture was fractionated on a 6% nondenaturing polyacrylamide gel.

### 2.9. Statistical Analysis

Where indicated, one-way ANOVA with Tukey post-hoc tests (GraphPad Prism) were used. All summary bar and line graphs are presented as mean +/− SEM, with significance denoted as follows *: $p<0.01$ and **: $p<0.001$.

## 3. Results

### 3.1. Oridonin inhibits HSC proliferation

Chemical structure of oridonin is shown in Figure 1A. The fibrogenic function of HSC is based on its activation and proliferation. To explore the antifibrotic effects of oridonin, the viability of LX-2 cells after oridonin treatment was first determined by Alamar Blue assay. As shown in Figures 1B and 1E, oridonin treatment significantly reduced LX-2 cell viability in a dose- and time-dependent manner. The $IC_{50}$ value was determined as ~7 M for 48 hour treatment from the dose-response curve using GraphPad Prism 5.0 software (GraphPad software, USA). A similar anti-proliferative effect of oridonin was observed in the activated rat hepatic stellate cell line HSC-T6 (Fig. 1C). Meanwhile, we compared oridonin with other natural compounds apigenin, curcumin, emodin, and quercetin for effects on LX-2 cell viability, and found that oridonin is the most potent anti-proliferative agent (data not shown). Next, C3A cells were used to test the cytotoxic effects of oridonin on normal human hepatocytes. C3A cells are a clonal derivative of the widely used human hepatocellular carcinoma HepG2 cell line and were selected for its better-differentiated hepatocyte phenotype [20]. As shown in Figure 1D, 10 M of oridonin treatment had no effects on C3A cell growth, and only 15% growth rate reduction at 12.5 M. For the following experiments, oridonin at 5 and 7.5 M were used to avoid cellular toxicity. Taken together, oridonin is capable of reducing proliferation of activated HSC without incurring apparent cytotoxic effects on normal human hepatocytes.

### 3.2. Oridonin induces S phase arrest in LX-2 cells

To explore the possible mechanism underlying the anti-proliferation activity of oridonin, cell cycle progression in LX-2 cells was determined using flow cytometry. As indicated in Figure 2A, oridonin treatment (5 and 7.5 mol/L, 24 h) promoted a dose-dependent increase in the percent of cells in S phase and a corresponding decrease in the percent of cells in $G_1$ phase compared with 0.1% DMSO treated control cells. Because the majority of cells were

in the $G_0$–$G_1$ phase under normal conditions, we did not synchronize cells before flow cytometry.

Next, we assessed the influence of oridonin on cell cycle regulatory proteins through Western blot analyses (Figs. 2B, 2C, 2D, and 2E). Oridonin treatment resulted in a down-regulation of Cdk4 and an up-regulation of p16, p21, and p53 in a time-dependent manner.

### 3.3 Oridonin promotes LX-2 cell apoptosis

To determine whether the decrease in cell viability in oridonin treated LX-2 cells was due to the induction of apoptosis, we examined oridonin treated LX-2 cell lysates with the Cell Death Detection ELISA assay. This assay measures the cytosolic histone fragments, which are a hallmark of apoptosis. As shown in Figures 3A and 3B, a dose-dependent increase of apoptotic cells was detected after 24-hour treatment; a time-dependent increase in apoptotic cells was observed with 7.5 M of oridonin treatment. This result was confirmed by Yo-pro-1 staining, which detects early apoptotic cells. As indicated in Figure 3C, while vehicle-treated control cells displayed negative staining of Yo-pro-1, treatment with oridonin led to positive Yo-pro-1 staining, indicating early apoptosis. The expression of apoptotic proteins was examined for the possible mechanism of oridonin induced apoptosis. As shown in Figures 3D and 3E, cleaved PARP was significantly increased in a time-dependent manner with 7.5 M of oridonin treatment, and cleaved caspase-9, but not caspase-3, was found to be increased with western blot analysis. In addition, Bcl-2 and Bax levels had no change in expression after treatment with 7.5 M of oridonin (data not shown).

### 3.4 Oridonin down-regulates endogenous α-SMA and ECM protein levels in LX-2 cells

The activation of HSC is one of the central pathophysiological mechanisms of hepatic fibrogenesis. HSC activation is characterized by overexpression of α-SMA as well as ECM proteins type I collagen and fibronectin. The effects of oridonin on endogenous expression of HSC activation marker α-SMA and ECM proteins were evaluated by Western blot assay. LX-2 cells were exposed to 7.5 M of oridonin for 14, 24, 48, and 72 hours and total protein was isolated for subsequent analysis. Oridonin treatment significantly decreased expression of type I collagen and α-SMA in a time-dependent manner (Figs. 4A and 4B). Fibronectin was increased slightly by oridonin in 14 hours, and then decreased constantly (Fig. 4C).

### 3.5 Oridonin blocks TGF-β signaling in LX-2 cells

TGF-β has been proven as a potent stimulator for ECM production in HSC [21]. We thereby examined the phosphorylation features of the Smad proteins, and further investigated the mechanism for the inhibition of TGF-stimulated ECMs by oridonin. As indicated in Figure 5A, TGF-β (2 ng/mL) potently induced Smad2/3 phosphorylation, pretreatment with oridonin inhibited TGF-β-induced Smad2/3 phosphorylation. As shown in Figures 5B and 5C, type I collagen and fibronectin were significantly up-regulated by TGF-β stimulation compared with vehicle treatment. Pretreatment with oridonin effectively decreased TGF-β-stimulated expression of type I collagen and fibronectin proteins. Transcriptional activation by Smads in many instances occurs via the direct binding to a cognate Smad-binding element (SBE) [22]. We performed EMSA assay to determine DNA binding activity of phosphorylated Smads in LX-2 cells. As shown in Figures 5D, TGF-β (2 ng/mL)

dramatically stimulated SBE DNA binding activity, pretreatment with oridonin significantly reduced SBE DNA binding.

## 4 Discussion

Oridonin has been studied for treatment of different cancers. To our knowledge, this is the first report characterizing oridonin's antifibrotic effect. Oridonin inhibits activated HSC proliferation in both a time- and dose-dependent fashion, and promoted S-phase arrest via p53/p21 pathway. Apoptosis of activated HSC was induced in a time- and dose-dependent manner after oridonin treatment. Importantly, oridonin suppressed endogenous expression of HSC activation marker α-SMA, ECM protein type I collagen, and fibronectin. Furthermore, oridonin significantly reduced the expression of TGF-β stimulated-ECM proteins compared to control in activated HSC. Because it has been shown as a relatively safe biological agent [11] and protective of liver tissue in an experimental rodent model [16], oridonin is a very promising natural compound to use in the development of hepatic fibrosis drugs.

Oridonin caused S-phase arrest in LX-2 cells and was associated up-regulation of p53 and p21expression. p53 plays an important role in S phase arrest and p53 up-regulation is a common response in many cell types with damaged DNA, as well as being a mediator of apoptosis [24]. p21, under transcriptional control of p53, is induced by cellular damage and interacts with a number of proteins involved in growth control. Upregulation of p21 results in growth arrest after cellular damage [25]. DNA fragmentation and Yo-pro-1 staining data indicate that oridonin induces apoptosis in HSC. Recent studies have proposed that oridonin may cause apoptosis via a caspase-3 independent pathway [13, 25]. Zhang and colleagues demonstrated that oridonin induced cell death in L929 cells was mediated through caspase-3 independent degradation of PARP [13]. Our data suggest this is a possible mechanism in LX-2 cells demonstrated by unchanged expression in cleaved caspase-3, and increased levels of cleaved caspase-9 and cleaved PARP.

The finding of decreases in both endogenous and TGF-β stimulated-ECM protein expression by oridonin is novel, indicating that oridonin is a promising antifibrogenic agent. TGF-β is a major stimulator for ECM production in HSC. TGF-β stimulation of HSC occurs via binding of TGF-β to its receptor which leads to phosphorylation of Smad2 and Smad3. Phosphorylated Smad 2/3 form a heteromeric complex with Smad4 and translocates into the nucleus to bind DNA and affect ECM gene transcription. Our results illustrate that oridonin affected Smad2/3 phosphorylation and Smad SBE nuclear DNA binding. The decrease of TGF-β stimulated-ECM protein expression is likely due to impaired transcriptional machinery (Fig 5D). Treatment of oridonin resulted in suppressed endogenous type I collagen, which is the major ECM component in fibrotic liver and is potently stimulated by TGF-β. Interestingly, the expression of fibronectin, which is another ECM component in fibrotic liver, was initially increased in 14 hours and then decreased significantly. Recent studies have shown that the roles of fibronectin are complicated in liver fibrosis. The continuous presence of fibronectin supports matrix integrity, both *in vitro* and *in vivo* [26, 27]. In contrast, deletion of fibronectin leads to an increase in stellate cell activation, both at baseline and after TGF-β stimulation, due to an increase in TGF-β bioavailability leading to a more pronounced fibrosis. These data indicate that fibronectin also controls the availability

of active TGF-β and protects the liver from an excessive TGF-β-mediated response [28]. The precise connection between oridonin treatment and fibronectin functions in hepatic fibrosis warrant deeper study.

In activated human and rat hepatic stellate cell lines, oridonin has demonstrated a significant ability to decrease hepatic fibrosis *in vitro*. Although these cell lines are very useful tools for liver fibrosis research, the antifibrotic role of oridonin will need to be confirmed *in vivo*. In addition, a better understanding of the mechanism of action of Oridonin in hepatic fibrosis will allow for the development of more potent and potentially safer analogs.

## Acknowledgments

## References

1. Neff GW, Duncan CW, Schiff ER. The current economic burden of cirrhosis. Gastroenterol Hepatol (N Y). 2011; 7:661–671. [PubMed: 22298959]

2. Lee UE, Friedman SL. Mechanisms of hepatic fibrogenesis. Best Pract Res Clin Gastroenterol. 2011; 25:195–206. [PubMed: 21497738]

3. Asahina K. Hepatic stellate cell progenitor cells. J Gastroenterol Hepatol. 2012; 27(Suppl 2):80–84. [PubMed: 22320922]

4. Lemoinne S, Cadoret A, El Mourabit H, Thabut D, Housset C. Origins and functions of liver myofibroblasts. Biochim Biophys Acta. 2013; 1832:948–954. [PubMed: 23470555]

5. Tsukamoto H, Zhu NL, Wang J, Asahina K, Machida K. Morphogens and hepatic stellate cell fate regulation in chronic liver disease. J Gastroenterol Hepatol. 2012; 27(Suppl 2):94–98. [PubMed: 22320925]

6. Liu Y, Wang Z, Kwong SQ, Lui EL, Friedman SL, et al. Inhibition of PDGF, TGF-beta, and Abl signaling and reduction of liver fibrosis by the small molecule Bcr-Abl tyrosine kinase antagonist Nilotinib. J Hepatol. 2011; 55:612–625. [PubMed: 21251937]

7. Lee SH, Seo GS, Park YN, Yoo TM, Sohn DH. Effects and regulation of osteopontin in rat hepatic stellate cells. Biochem Pharmacol. 2004; 68:2367–2378. [PubMed: 15548383]

8. Ramm GA, Shepherd RW, Hoskins AC, Greco SA, Ney AD, et al. Fibrogenesis in pediatric cholestatic liver disease: role of taurocholate and hepatocyte-derived monocyte chemotaxis protein-1 in hepatic stellate cell recruitment. Hepatology. 2009; 49:533–544. [PubMed: 19115220]

9. Xu W, Sun J, Zhang TT, Ma B, Cui SM, et al. Pharmacokinetic behaviors and oral bioavailability of oridonin in rat plasma. Acta Pharmacol Sin. 2006; 27:1642–1646. [PubMed: 17112421]

10. Chen G, Wang K, Yang BY, Tang B, Chen JX, et al. Synergistic antitumor activity of oridonin and arsenic trioxide on hepatocellular carcinoma cells. Int J Oncol. 2012; 40:139–147. [PubMed: 21947421]

11. Ding C, Zhang Y, Chen H, Yang Z, Wild C, et al. Oridonin Ring A-Based Diverse Constructions of Enone Functionality: Identification of Novel Dienone Analogues Effective for Highly Aggressive Breast Cancer by Inducing Apoptosis. J Med Chem. 2013

12. Wang H, Ye Y, Chui JH, Zhu GY, Li YW, et al. Oridonin induces G2/M cell cycle arrest and apoptosis through MAPK and p53 signaling pathways in HepG2 cells. Oncol Rep. 2010; 24:647–651. [PubMed: 20664969]

13. Zhang CL, Wu LJ, Tashiro S, Onodera S, Ikejima T. Oridonin induces a caspase-independent but mitochondria- and MAPK-dependent cell death in the murine fibrosarcoma cell line L929. Biol Pharm Bull. 2004; 27:1527–1531. [PubMed: 15467189]

14. Ding C, Zhang Y, Chen H, Yang Z, Wild C, et al. Novel nitrogen-enriched oridonin analogues with thiazole-fused A-ring: protecting group-free synthesis, enhanced anticancer profile, and improved aqueous solubility. J Med Chem. 2013; 56:5048–5058. [PubMed: 23746196]

15. Ding C, Zhang Y, Chen H, Wild C, Wang T, et al. Overcoming synthetic challenges of oridonin A-ring structural diversification: regio- and stereoselective installation of azides and 1,2,3-triazoles at the C-1, C-2, or C-3 position. Org Lett. 2013; 15:3718–3721. [PubMed: 23834026]

16. Zhou GB, Kang H, Wang L, Gao L, Liu P, et al. Oridonin, a diterpenoid extracted from medicinal herbs, targets AML1-ETO fusion protein and shows potent antitumor activity with low adverse effects on t(8;21) leukemia in vitro and in vivo. Blood. 2007; 109:3441–3450. [PubMed: 17197433]

17. Xu L, Hui AY, Albanis E, Arthur MJ, O'Byrne SM, et al. Human hepatic stellate cell lines, LX-1 and LX-2: new tools for analysis of hepatic fibrosis. Gut. 2005; 54:142–151. [PubMed: 15591520]

18. Hamid R, Rotshteyn Y, Rabadi L, Parikh R, Bullock P. Comparison of alamar blue and MTT assays for high through-put screening. Toxicol In Vitro. 2004; 18:703–710. [PubMed: 15251189]

19. Nociari MM, Shalev A, Benias P, Russo C. A novel one-step, highly sensitive fluorometric assay to evaluate cell-mediated cytotoxicity. J Immunol Methods. 1998; 213:157–167. [PubMed: 9692848]

20. Kelly JH, Darlington GJ. Modulation of the liver specific phenotype in the human hepatoblastoma line Hep G2. In Vitro Cell Dev Biol. 1989; 25:217–222. [PubMed: 2466032]

21. Shi YF, Zhang Q, Cheung PY, Shi L, Fong CC, et al. Effects of rhDecorin on TGF-beta1 induced human hepatic stellate cells LX-2 activation. Biochim Biophys Acta. 2006; 1760:1587–1595. [PubMed: 17067743]

22. Dennler S, Itoh S, Vivien D, ten Dijke P, Huet S, et al. Direct binding of Smad3 and Smad4 to critical TGF beta-inducible elements in the promoter of human plasminogen activator inhibitor-type 1 gene. EMBO J. 1998; 17:3091–3100. [PubMed: 9606191]

23. Liu Q, Wang X, Zhang Y, Li CJ, Hu LH, et al. Leukamenin F suppresses liver fibrogenesis by inhibiting both hepatic stellate cell proliferation and extracellular matrix production. Acta Pharmacol Sin. 2010; 31:839–848. [PubMed: 20562900]

24. Ciciarello M, Mangiacasale R, Casenghi M, Zaira Limongi M, D'Angelo M, et al. p53 displacement from centrosomes and p53-mediated G1 arrest following transient inhibition of the mitotic spindle. J Biol Chem. 2001; 276:19205–19213. [PubMed: 11376010]

25. Cui Q, Yu JH, Wu JN, Tashiro S, Onodera S, et al. P53-mediated cell cycle arrest and apoptosis through a caspase-3- independent, but caspase-9-dependent pathway in oridonin-treated MCF-7 human breast cancer cells. Acta Pharmacol Sin. 2007; 28:1057–1066. [PubMed: 17588343]

26. Sottile J, Hocking DC. Fibronectin polymerization regulates the composition and stability of extracellular matrix fibrils and cell-matrix adhesions. Mol Biol Cell. 2002; 13:3546–3559. [PubMed: 12388756]

27. Bentmann A, Kawelke N, Moss D, Zentgraf H, Bala Y, et al. Circulating fibronectin affects bone matrix, whereas osteoblast fibronectin modulates osteoblast function. J Bone Miner Res. 2010; 25:706–715. [PubMed: 19821765]

28. Kawelke N, Vasel M, Sens C, Au A, Dooley S, et al. Fibronectin protects from excessive liver fibrosis by modulating the availability of and responsiveness of stellate cells to active TGF-beta. PLoS One. 2011; 6:e28181. [PubMed: 22140539]
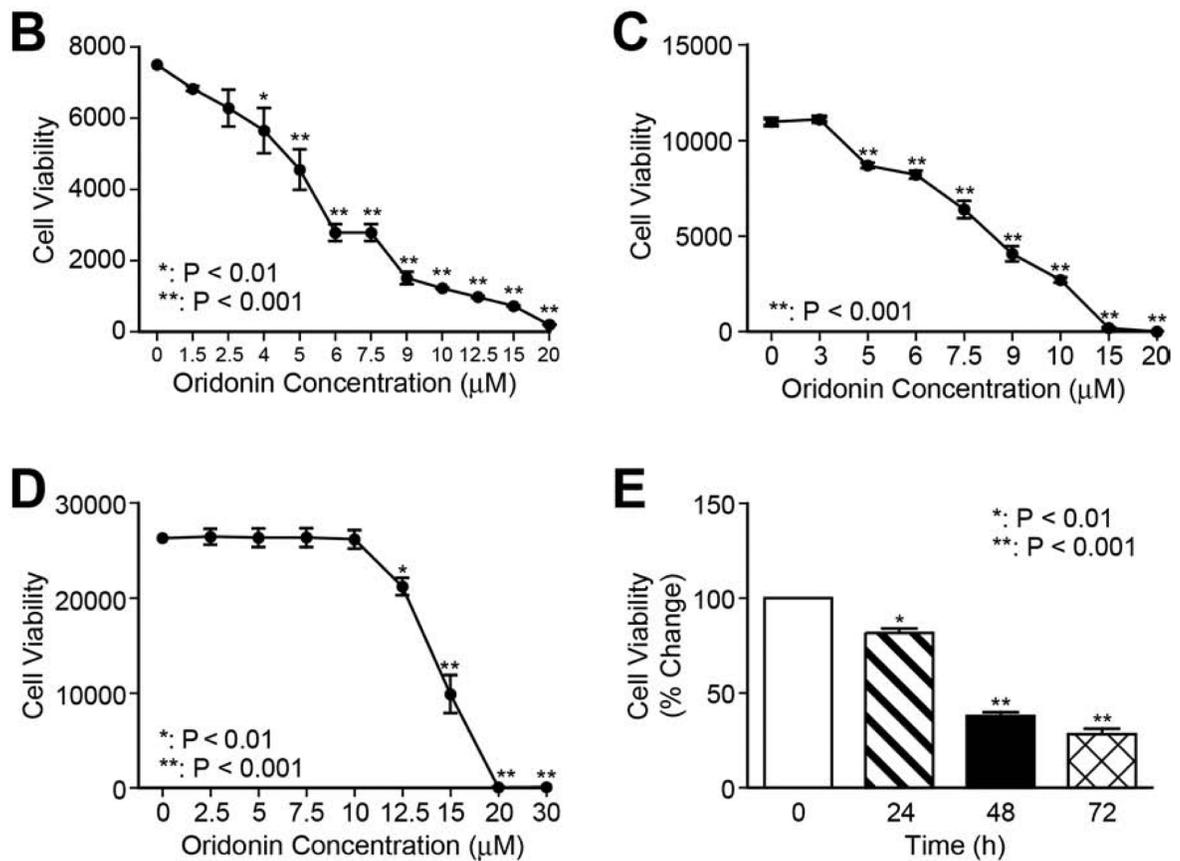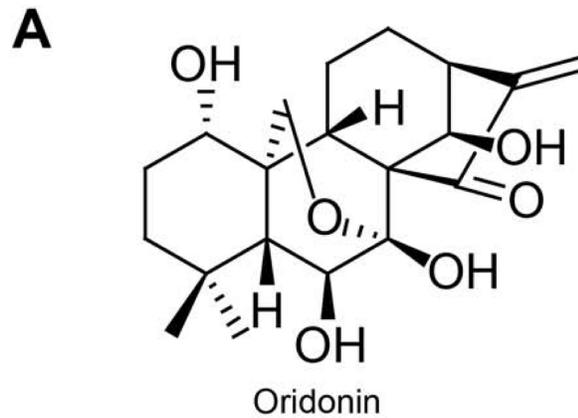
**Fig. 1. Oridonin suppresses HSC proliferation**

Chemical structure of oridonin (A). LX-2 cells (B), HSC-T6 cells (C) and C3A hepatocytes (D) were treated with a series of concentrations of oridonin for 48 hours, and cell viability was determined using Alamar Blue assay. (E) LX-2 cells were treated with 7.5 μmol/L of oridonin for 24, 48, and 72 hours; cell viability was measured by Alamar Blue assay. P-values shown compared to vehicle (0.1% DMSO, 0 μmol/L). The results are representative of at least three independent experiments.
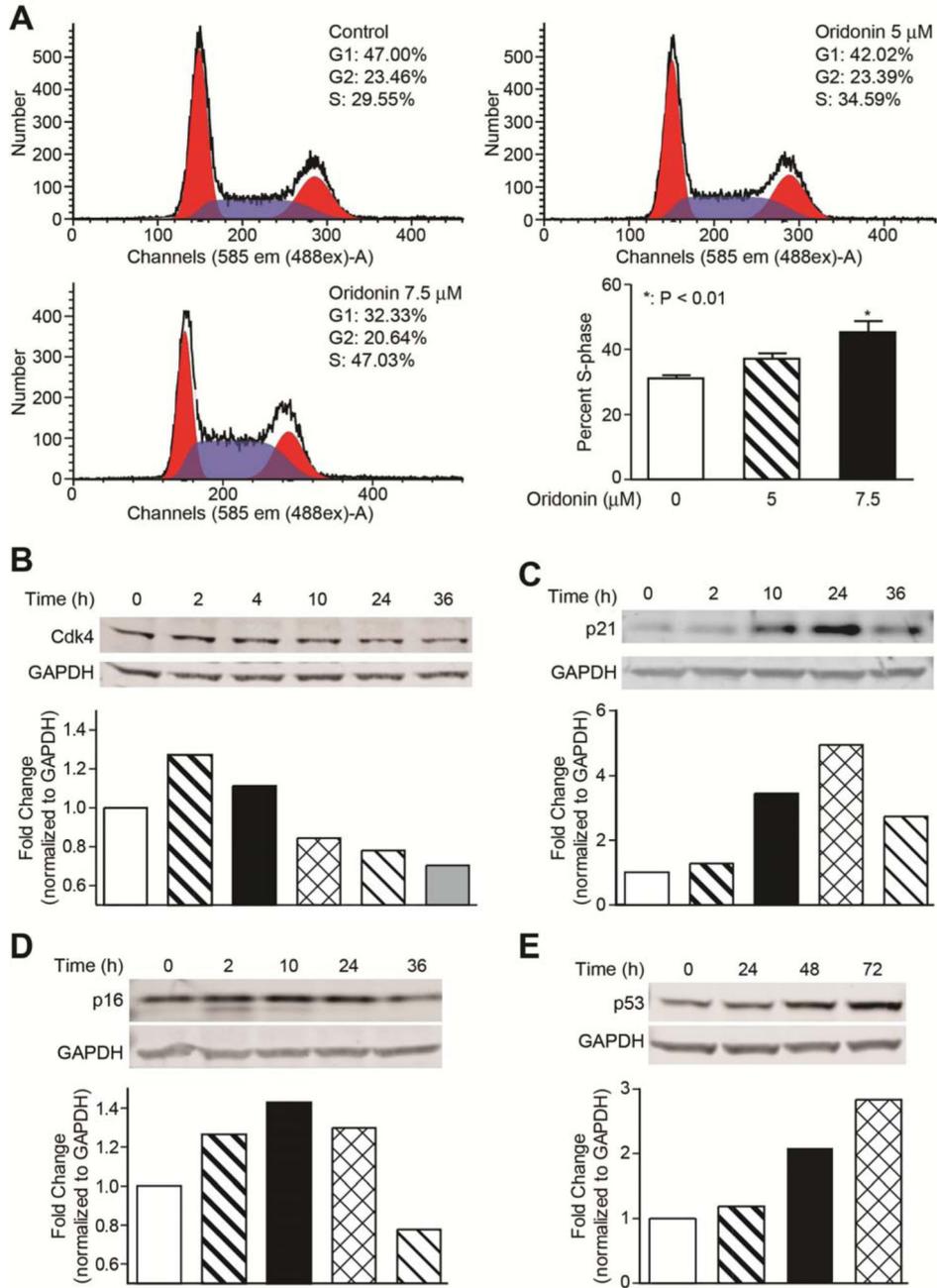
**Fig. 2. Oridonin induces LX-2 cell cycle arrest**

(A) Oridonin induces S-phase cell cycle arrest. LX-2 cells were treated with oridonin (0, 5, and 7.5 µmol/L) for 24 hours. Cells were stained with propidium iodide and analyzed by flow cytometry as described in Methods. The experiments were repeated three times and representative data are shown. (B), (C), (D), and (E) Oridonin affects cell cycle regulatory proteins. LX-2 cells were treated with vehicle (0.1% DMSO) or oridonin (7.5 µmol/L) for indicated time points. Whole cell lysates were analyzed by Western blot with antibodies for
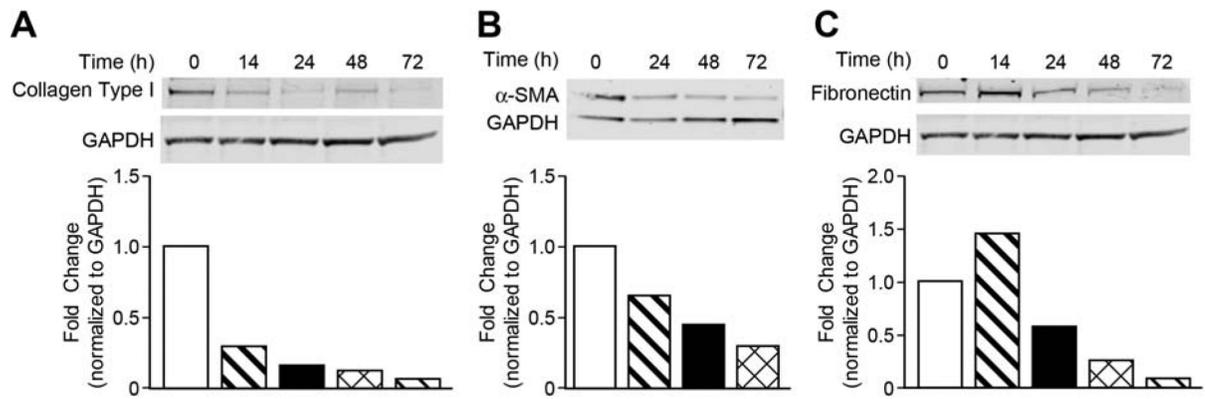
Cdk4, p21, p16, and p53. GAPDH was used as loading control. Densitometric analyses of bands were quantified and data expressed as fold change of control normalized to GAPDH.
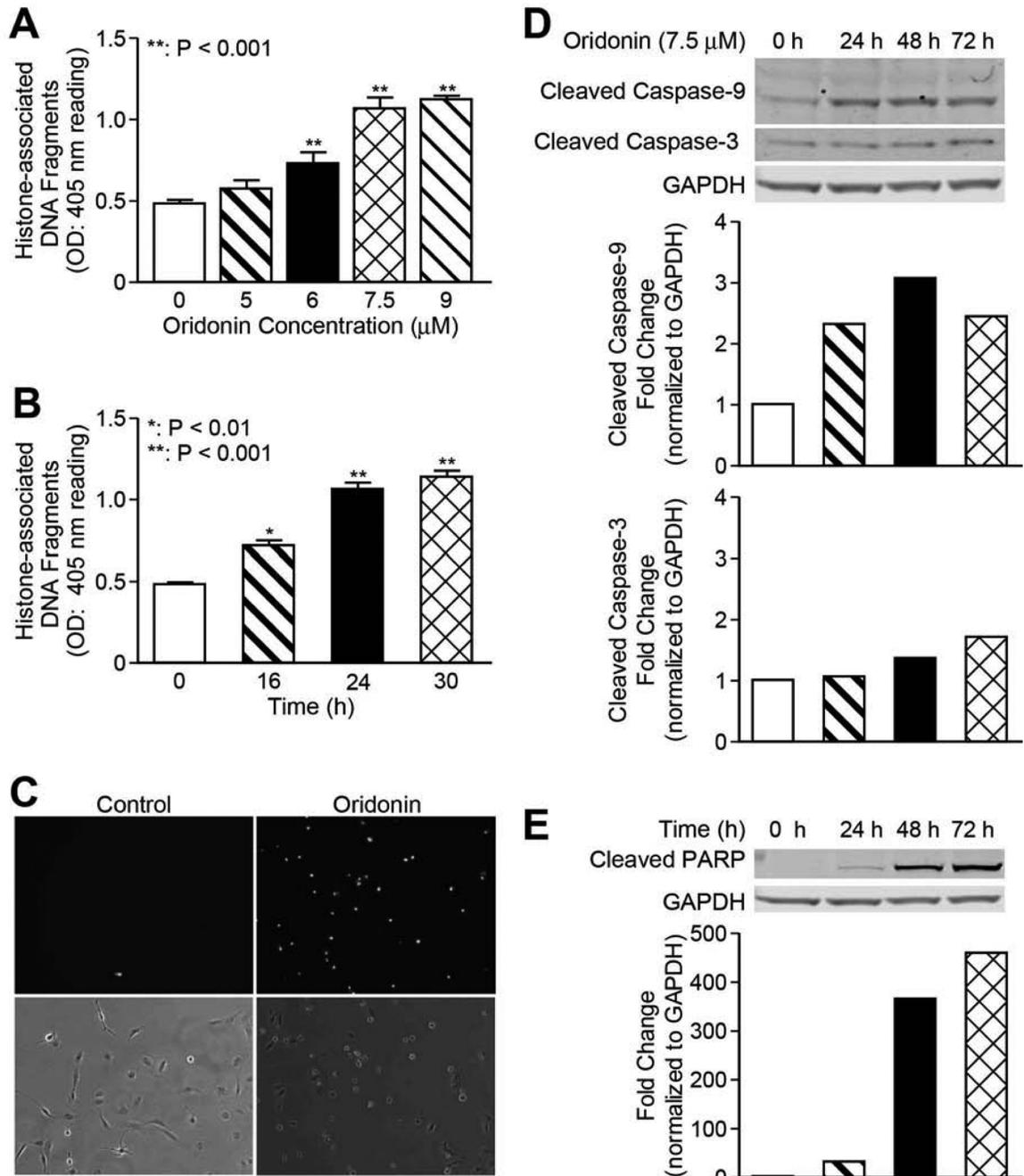
**Fig. 3. Oridonin promotes LX-2 cell apoptosis**
LX-2 cells were incubated with different concentrations or time points as indicated. Apoptosis by oridonin was evaluated either by Cell Death detection ELISA (each conducted in triplicate) (A) and (B), or Yo-Pro-1 staining (C). Whole cell lysates were analyzed by Western blot with antibodies for cleaved caspase-3 and cleaved caspase-9 (D), cleaved-PARP (E). GAPDH was used as loading control. Densitometric analyses of bands were quantified and data expressed as fold of control normalized to GAPDH. The results are representative of at least three independent experiments.

**Fig. 4. Oridonin suppresses α-SMA and ECM protein expression**
LX-2 cells were incubated with oridonin (7.5 μmol/L) at time points as indicated. Whole cell lysates were analyzed by Western blot with antibodies for Type I collagen (A), α-Smooth muscle actin (B) and fibronectin (C). GAPDH was used as loading control. Densitometric analyses of bands were quantified and data expressed as fold change of control normalized to GAPDH. The results are representative of at least three independent experiments.
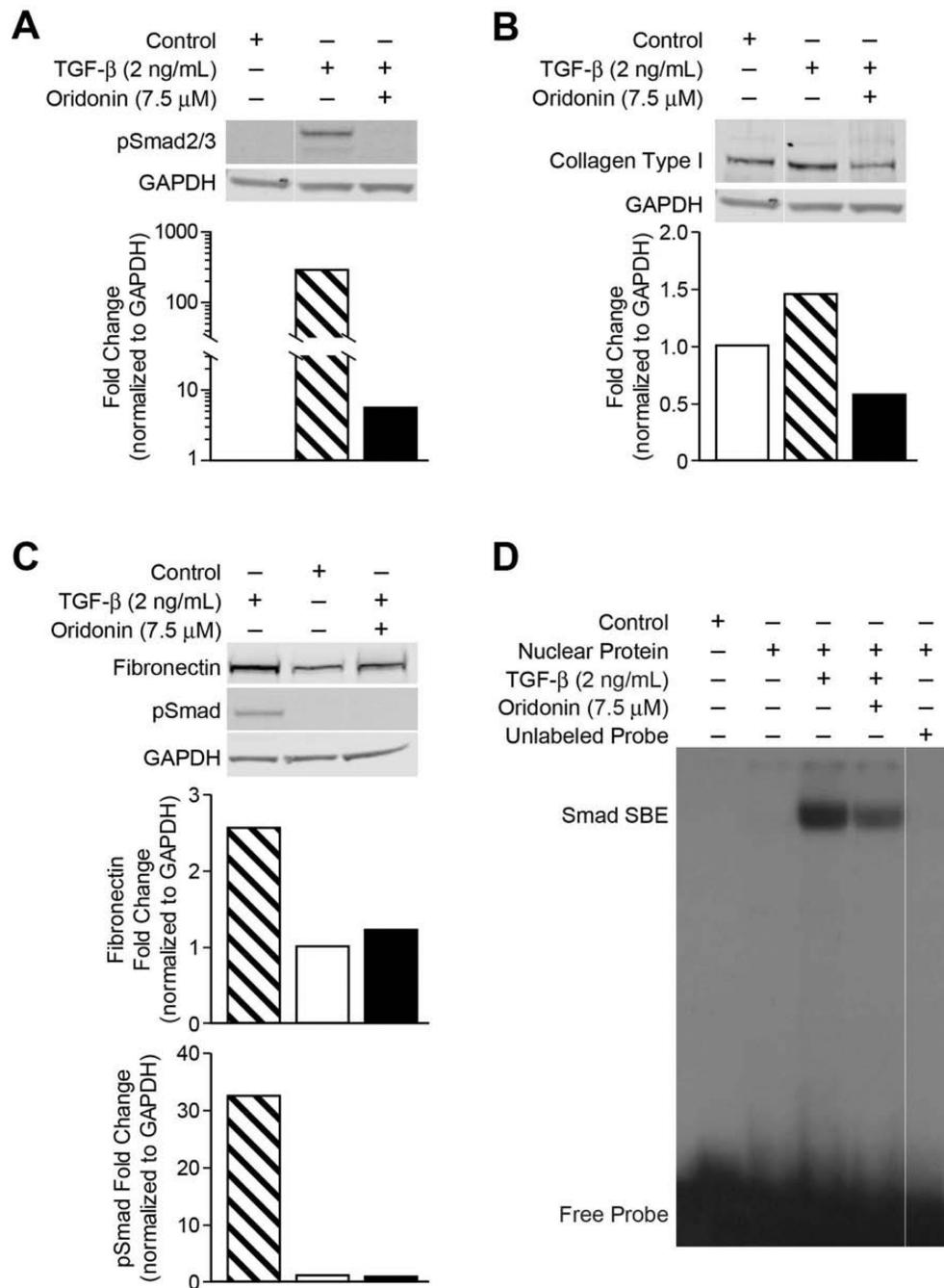
**Fig. 5. Oridonin inhibits TGF-β induced pSmad activity and ECM**

LX-2 cells were preincubated with oridonin (7.5 μmol/L) for 2 hours and then treated with TGF-β (2 ng/mL) for 18 hours, whole cell lysates were analyzed by Western blot with antibodies for phosphorylated-Smad2/3 (A) and type I collagen (B), fibronectin (C). GAPDH was used as loading control. Densitometric analyses of bands were quantified and data expressed as fold change of control normalized to GAPDH. (D) LX-2 cells were pretreated with 7.5 mol/L of oridonin for 1 hour and then treated with TGF-β (2 ng/mL) for

1 hour. Nuclear proteins were extracted and analyzed by EMSA with $^{32}$P-labeled SBE probe described in experiment procedures.